UNCLASSIFIED

AD NUMBER
AD366593

CLASSIFICATION CHANGES

TO: unclassified

FROM: confidential

LIMITATION CHANGES

TO:

Approved for public release, distribution unlimited

FROM:

Distribution authorized to U.S. Gov't. agencies and their contractors; Administrative/Operational Use; 15 Sep 1965. Other requests shall be referred to Naval Research Laboratory, Washington, DC. 20375.

AUTHORITY

31 Dec 1969, GDS, DoD 5200.1-r; NRL ltr, 22 Jan 2004

GENERAL DECLASSIFICATION SCHEDULE

IN ACCORDANCE WITH
DOD 5200.1-R & EXECUTIVE ORDER 11652

THIS DOCUMENT IS:

CLASSIFIED BY_____

Subject to General Declassification Schedule of

Executive Order 11652-Automatically Downgraded at

2 Years Intervals- DECLASSIFIED ON DECEMBER 31, *1969*

BY
Defense Documentation Center
Defense Supply Agency
Cameron Station
Alexandria, Virginia 22314

SECURITY

MARKING

The classified or limited status of this report applies
to each page, unless otherwise marked.
Separate page printouts MUST be marked accordingly.

CONFIDENTIAL

Test of
Project ARTEMIS Acoustic Source

R. H. FERRIS

Electrical Applications Branch
Sound Division

September 15, 1965

CONFIDENTIAL

SECURITY

CONFIDENTIAL

CONTENTS

CONFIDENTIAL

ABSTRACT

The ARTEMIS acoustic source has been completed by the addition of the top row of five transducer modules. Concurrent with the installation of the additional transducer elements, the electrical connection to the elements was modified from a series-parallel connection to an all-parallel configuration. The modification was performed to reduce the effects of acoustic interactions, which severely limited the power handling capability.

Tests of the completed and modified source were conducted during July 1964 in Northwest Providence Channel. Results of the tests indicated a substantial increase in power handling capacity had been achieved with a maximum permissible source level, at the optimum frequency, of 148 decibels versus one dyne per square centimeter at one yard for pulsed sinusoidal excitation. The maximum allowable power, however, is a marked function of frequency, being especially limited at the upper end of the operating band. A non-rectilinear mode of vibration in the elements, as well as variations in loading due to acoustic interactions, contributed to the limitation of allowable power.

Tests with phase modulated pseudorandom noise excitation revealed that a lower power level was required in this mode of operation than with pulsed sinusoids.

PROBLEM AUTHORIZATION

ONR RS 046
NRL problem 55S02-11

PROBLEM STATUS

This is an interim report on one phase of this project. Work is continuing.

INTRODUCTION

The ARTEMIS acoustic source was completed by the addition of the top row of five transducer modules, resulting in a rectangular plane array 33 feet in width and 50 feet high. The transducer array is composed of 1440 variable reluctance elements. The elements, which are cubicle in shape and approximately 11 inches on a side, are installed in module frames containing 12 rows of six elements each. Twenty modules are arranged in four rows of five modules each on the supporting array structure. A view of the completed array installed on the USNS MISSION CAPISTRANO (T-AG 162) is shown in Figure 1.

Concurrent with the installation of the additional transducer elements, the electrical connection to all elements was modified from the previous arrangement, in which groups of six elements were connected in series and all series groups connected in parallel, to the present configuration, in which all elements are parallel connected. This was accomplished by the installation of paralleling transformers on the array structure behind each transducer module. The transformers were required to preserve the impedance compatibility between the transducer modules and existing circuitry. The squashed tubes, which provide pressure release backing for the elements, were also replaced by tubes of an improved design. The modifications were performed by Hudson Laboratories of Columbia University. A view of one of the installed transformer tanks is shown in Figure 2, and Figure 3 illustrates the arrangement of one row of tanks on the array structure.

Tests of the completed and modified source were conducted during the period 19 July through 3 August 1964 at Northwest Providence Channel in the area bounded by 77° 30' and 79°00' W longitude, and 25° 50' and 26° 40' N latitude.

PURPOSE

These tests were conducted to determine the maximum allowable input power as a function of frequency. Since the power limit is imposed by the mechanical fatigue strength of the transducer element springs, which support an inner mass inside the outer mass, the tests were designed to obtain a statistical sample of spring deflections and element mass displacement from which the limiting power levels could be deduced.

Although acoustic response measurements were not included as an objective of these tests, a few on-axis measurements at selected frequencies were obtained.

EXPERIMENTAL PROCEDURE

One specially instrumented transducer module was installed in module position number two; that is, the second position from the left in the top row when facing the front of the array. During the course of the tests, the special module was moved sequentially to positions 8, 14, 20, and 11, as shown in Figure 4. At each position, transducer displacement data were recorded as a function of frequency and certain spring deflections examined with broadband signal excitation. When these tests had been completed and the data examined, the array was driven at a maximum safe power level for an accumulated time of two hours at each of several frequencies within the operating band. The transducer impedance was measured concurrently with the displacement tests. The array was also driven at varying power levels to ascertain its linearity characteristics. At the conclusion of all displacement tests, the transmitting response at each of several frequencies was measured on the acoustic axis of the source. The monitoring hydrophone was suspended from a small boat which was tethered to the source ship at a range of approximately 300 feet. The acoustic axis was located by searching in azimuth and depth for maximum response. Range to the hydrophone was measured acoustically. Short continuous wave pulses were used to enable time separation of the direct and surface-reflected paths. During all displacement tests the array was submerged to a depth of 600 feet to its center. A source depth of 250 feet was used for the acoustic measurements.

INSTRUMENTATION

The specially instrumented module contained 32 special elements, each fitted with two internal accelerometers, one at the top edge and one at the bottom edge of the inner mass, and one external accelerometer in the center of the radiating face. The remainder of the test module was completed with 40 normal Massa type TR-11C transducer elements. The elements were arranged in the test module as shown in Figure 5. Each of the 32 special elements was reversed in the module, having its power cable termination toward the front of the array. Element reversal was necessary in order to permit the attachment of an accelerometer on the radiating face in a tapped hole provided directly beneath the power cable termination. Proper vibrational phase of each reversed element was maintained by rotating the power plug 180 degrees relative to its receptacle, thus reversing the phase of the driving signal.

2   CONFIDENTIAL

A pressure housing was bolted on the back side of the test module. This enclosure contained a preamplifier and the necessary control circuitry to sequentially sample each of the 96 accelerometers attached to the transducer elements and to transmit their amplified outputs to the surface. In addition, the enclosure contained five adder circuits which combined the outputs of five selected pairs of accelerometers. Each pair consisted of an accelerometer on the radiating face of an element and one of the two accelerometers on the inner mass of the same element. The adder circuits enabled the continuous observation of spring deflections in five selected elements while the source was excited with pseudorandom noise. When sine wave excitation was used, spring deflections were measured in all specially instrumented elements by sequentially sampling the output phase and amplitude of each individual accelerometer and computing the spring deflections by vector addition of appropriate pairs. In this manner, spring deflections and element mass displacements were sampled from 32 special elements in each of the five test module positions at frequencies of 350, 355, 360, 365, 370, 375, 380, 382.5, 385, 387.5, 390, 392.5, 395, 400, 402.5, 405, 407.5, 410, 412 5, 415, 417.5, 420, 422.5, 425, 430, 435, 440, 445, 447.5, 450, 460, 470, 480, 490, and 500 cycles per second. The current into the transducer was held constant at 50 amperes except at frequencies higher than 445 cycles per second where it was reduced to 25 amperes. The elements were polarized with ten amperes direct current.

The array was also driven with a phase modulated pseudorandom noise sequence of degree 12, code number one.[1] The phase modulation consisted of reversing the phase of a 400 cycle per second signal at coded intervals in multiples of four cycles. The output of the generator was passed through a filter having a bandwidth of 100 cycles per second centered at 400 cycles per second. A second pseudorandom noise source, consisting of a 17-stage shift register with a clock rate of 3200 cycles per second and a 100 cycle per second bandpass filter, was employed. However, a malfunction was apparently present which left the exact code sequence in doubt. Oscillographic and magnetic tape recordings were made of the outputs of each of the five spring deflection adder circuits at each of the five positions of the test module while the array was driven from each of the two pseudorandom noise generators. External and internal mass displacement waveforms were also recorded for several selected elements. The outputs of the accelerometer and adder circuits were processed through a 12 decibel per octave filter prior to recording

----

1. W. Wesley Peterson, Error-Correcting Codes, M.I.T. Press, 1961

in order to convert voltage amplitudes proportional to acceleration to a
voltage amplitude proportional to displacement.

A view of data recording instrumentation aboard the USNS MISSION
CAPISTRANO is shown in Figure 6.

RESULTS

Impedance

The results of electrical impedance measurements of the transducer
array at the ship termination of the connecting cable are plotted in
Figure 7. The illustrated data were obtained with the array submerged
to a depth of 600 feet during the first experiment. The impedance was
measured during each of the four succeeding experiments in which the
test module was moved to four successive positions in the array. No
significant change in impedance was observed throughout the experiments.

Acoustic Response

The free-field current, voltage, and power response of the transducer
are plotted in Figure 8. Acoustic measurements were obtained at each
of eight frequencies with the array submerged to a depth of 250 feet and
with an electrical power input of approximately 200 kilowatts.

Loading

An approximate average loading ratio for the entire array can be computed
from the ratio of radiated power to that power which would be radiated
by a uniformly vibrating piston of equal size having a displacement equal
to the measured average displacement and radiating into a unit ρcA real
load. This computation produces an accurate result only when the
velocity is uniform over the face of the array. Figure 9 illustrates the
loading ratio computed for the ARTEMIS source array. The average dis-
placement was computed for approximately a ten percent sample of the
elements. Values of loading ratio for frequencies above 430 cycles per
second are questionable due to the nonuniform velocity distribution at
these frequencies.

Distribution of Displacements

The uniformity of displacements of the radiating faces from element to element varies as a function of frequency. The acoustic interaction among the elements results in spatial variation in radiation loading over the face of the array. Since all elements are electrically connected in parallel, they all are driven by the same voltage. Since the acoustic loading modifies the electrical impedance, the electrical power inputs to the elements will vary with the acoustic load. The variation in both input power and load results in a diversity of element displacements. The effect of interactions is more pronounced at the upper end of the frequency band. This is a consequence of the manner in which the displacement response is affected by loading. To illustrate this effect, the transducer spring deflections resulting from a constant driving voltage of 100 volts are plotted as a function of frequency in Figure 10. The data from which the solid line is plotted were obtained from measurements on a single unloaded element in air. The dashed line was obtained from an average of the characteristics of all of the specially instrumented elements in water. It can be seen that a completely unloaded element connected in parallel with an element having average loading would experience approximately the same spring deflection as the loaded element over all frequencies in the operating band. In the region of the response pole, however, the spring deflection is strongly controlled by loading. For the conditions of loading illustrated in Figure 10, there would appear to be no problem within the operating band for parallel connected elements. However, elements having a large mass load with only a small resistive component exhibit a minimum impedance at a lower frequency than the illustrated unloaded element, and the frequencies at which the elements are sensitive to loading can be extended downward into the operating band. For this reason, a few elements exhibit extremely large deflections at the upper end of the band.

The observed distribution of outer mass displacements for six frequencies within the operating band is illustrated in Figure 11. Displacements have been normalized to the mean displacement at each frequency. The uniformity of displacements progressively deteriorates at frequencies above 430 cycles per second. Similar distributions of transducer spring deflections are illustrated in Figure 12. These distributions also show a deterioration at the high frequency end of the band. In addition, a band of frequencies in the vicinity of 400 cycles per second exhibits poor distributions. It will be shown that the poor distributions at midband are caused by a rotary mode of vibration in the elements.

Since mechanical fatigue of the transducer springs limits the power handling capability of these elements, the electrical power input to the array is limited to that value which does not produce excessive spring deflections in those elements having the largest deflections. At 450 cycles per second, the spring deflections have values ranging from 0.2 to 2.5 times the mean deflection. The power input must be reduced approximately eight decibels below that value which would have been allowable had the spring deflections been uniform. At 460 cycles per second the power handling capability is degraded by approximately ten decibels by the dispersion of spring deflections. Although 460 cycles per second is not within the operating band, care must be exercised to avoid exciting the transducer array at this frequency.

The mean value of spring deflections for all sampled elements is plotted as a function of frequency in Figure 13, along with the maximum observed deflection at each frequency. All values have been normalized to 100 kilowatts electrical power input. The high dispersion of spring deflections at the upper end of the frequency band results in a high ratio of maximum-to-mean values. The high ratio at 395 cycles per second is caused by a rotational mode of vibration.

To exemplify the observed spring deflections in an individual element, the data obtained from element 8-1 have been plotted in Figures 14 and 15 for two positions of the test module. Each illustration contains two curves, one labeled "Top" and one labeled "Bottom". These refer respectively to the deflections computed by vectorially adding the output of the accelerometer attached to the upper edge of the inner mass to the output of the external accelerometer and that of the accelerometer attached to the lower edge of the inner mass to the output of the external accelerometer. Figure 14 illustrates data from test module position 2, which is the second position from the left in the top row of modules. The data illustrated in Figure 15 were obtained with the test module in position 11, which is the extreme left position in the third row from the top. In the latter position, element 8-1 is on the extreme left edge of the array. In both cases, the input current to the array was 50 amperes at each frequency. For frequencies from 350 to 380 cycles per second there are relatively small differences between the top and bottom deflections and between deflections in the two positions, indicating little or no rotary motion in a vertical plane and very small sensitivity to loading if it is assumed that there is a difference in loading in the two positions. In the frequency range from 380 to 420 cycles per second, the dissimilarity of top and bottom deflections indicates severe rotary motion in a vertical plane. This particular element exhibits a larger than average rotary mode.

At frequencies above 420 cycles per second the top and bottom deflections are nearly equal, signifying an absence of rotary motion. In this frequency range, however, the deflections for the two module positions vary markedly as a consequence of the high sensitivity to loading at the upper end of the band.

Rotary Vibrational Mode

The data from the three accelerometers on each of the instrumented elements were processed to obtain the angle of rotation occurring between the elements' inner and outer masses. Illustrative of the rotary motion experienced by elements is the rotary response of elements in positions 3-1, 8-1, and 3-4, which are plotted in Figures 16 through 18. The high Q resonances of the rotational modes of these elements produce peak rocking angles which can result in greatly increased spring deflections. One minute of arc can result in an increase in spring deflection of nearly one mil. Since the rotary motion is not acoustically coupled into the water, it degrades the power handling capability of the elements. The average and maximum values of rocking angles for all sampled elements are plotted on a reduced scale in Figure 19. An inspection of the data has revealed that the rocking angle of an element is not affected by the acoustic loading as evidenced by nearly identical rotary responses as an element is operated in various positions in the array.

Later experiments in the laboratory with an element loaded by placing it in a box filled with gravel indicated that the only effect of an external load on the rocking motion was a moderate decrease in the Q of the rotary resonance. However, when the element was asymmetrically loaded with gravel covering only the lower portion of the element, the rocking motion was aggravated. This would suggest that any asymmetric loading introduced in the transducer array, such as from asymmetrically placed pressure release tubes or from foreign material becoming wedged under the elements might degrade performance by increasing the rocking motion.

Power Limitation

Since the power limitation for these elements is imposed by fatigue of the element springs, the maximum allowable electrical power input can be extrapolated from the maximum observed deflection at a known input power at each frequency. Manufacturer's tests and experimental results indicate that a peak-to-peak deflection of 0.01 inches is approximately

CONFIDENTIAL

the maximum safe value. The curve of maximum allowable input power
versus frequency plotted in Figure 20 represents the power input required
to produce a maximum spring deflection of 7.08 thousandths of an inch in
the sampled elements. The choice of 7.08 milinches for the limiting
deflection results from the application of a three decibel safety factor to
the 10 milinch maximum allowable deflection. A safety factor of three
decibels is estimated to be required to account for the size of the statisti-
cal sample and to allow for the transient overshoot when the input signal
is pulsed. A further study of transient behavior of the elements is needed
to define more precisely the required safety factor. The corresponding
maximum allowable voltage input to the driving amplifiers is plotted in
Figure 21. Since the voltage gain of the amplifiers can be adjusted to
various values, the input voltage is given as a relative value referenced
to the maximum allowable input voltage at 380 cycles per second for the
particular amplifier gain employed during the tests. The amplifier input-
output relations were obtained with a constant voltage input over the
frequency range to two amplifiers connected in parallel to the transducer
load. The value of input voltage used in the test was selected such that
the maximum allowable input power was not exceeded at any frequency.
The data plotted in Figure 21 have been extrapolated to the value required
to produce the maximum input power at each frequency.

The maximum input power data have been combined with the data of
acoustic measurements to produce the values of maximum available source
level plotted in Figure 22. This curve includes the three decibel safety
factor introduced in the maximum allowable power input data and applies
to pulsed sinusoidal transmissions in which the signal input to the ampli-
fiers is passed through a filter having a bandwidth of 100 cycles per
second.

Linearity

Linearity of array characteristics was examined by operating at power
levels from 50 to 400 kilowatts in 50 kilowatt increments at 415 cycles
per second. Neither the element mass displacements nor the components
of array impedance displayed any significant nonlinearity.

Endurance

At the conclusion of the experiments an endurance run was made for an
accumulated time of eight hours. This consisted of two hours each at
350, 415, 430, and 450 cycles per second at power levels of 200, 400,

300, and 120 kilowatts electrical input. The power levels employed were based on a preliminary analysis of the data. It was later discovered that an error was introduced in the measurement of inner mass displacement, and hence, spring deflections, by capacitive coupling between the power circuits and the accelerometers within the elements. Measurements were made of the magnitude of this effect and the errors were removed analytically in the final data analysis. Since the preliminary analysis did not recognize this error, the endurance runs at 430 and 450 cycles per second were conducted at higher power levels than are now recommended. A check of the elements following the endurance tests revealed that two elements had been damaged. Of the 240 new squashed tubes on the array, three failed during the test.

Pseudorandom Noise

When the array was energized with phase modulated pseudorandom noise, an examination of the oscillographic records of element mass displacements revealed a very nearly linear relationship between the signal voltage waveform and the external mass displacement. The spring deflections, however, showed no recognizable correspondence. Large peak values of deflection occurred at apparently random intervals in the sequence. Measurements of the deflection peak values indicated that the maximum allowable rms current input is 85 amperes. This results in a source level of approximately 140 decibels.

CONCLUSIONS

The modification of the electrical connection of elements in the ARTEMIS source array from a series-parallel to an all-parallel configuration has resulted in greatly improved performance with respect to available source level. The maximum allowable source level at the optimum frequency, 420 cycles per second, is 148 decibels referenced to one dyne per square centimeter at one yard for pulsed sinusoidal excitation. This compares with a maximum source level of 136 decibels at 405 cycles per second prior to completion and modification of the array.

The maximum allowable power input, which is restricted by the mechanical endurance of the transducer element springs, varies markedly with frequency and is drastically reduced at the upper end of the frequency band. Acoustic interactions cause a variation in loading from element to element at all frequencies. With parallel connection of elements, which

results in a like voltage being applied to all elements, the element spring deflections are insensitive to acoustic loading over most of the operating band. At the upper end of the band, however, those elements with a predominantly mass loading undergo large deflections relative to the resistively loaded elements. This accounts for the drastic power limitation at high frequencies. A further limitation on power is imposed by a nonrectilinear mode of vibration of the transducer elements in which the inner mass rotates relative to the outer mass. This mode of vibration increases spring deflections but does not couple acoustic energy into the water. Most elements have a high Q resonance in this mode in the vicinity of 400 cycles per second.

Excitation of the source by phase modulated pseudorandom noise results in a high peak to rms ratio of spring deflection even though the ratio is low for both the input signal and the displacement of the radiating face. This, plus the fact that with noise-like signals the energy is spread over the band including those frequencies with less than optimum allowable power input, degrades the available source level for noise relative to sinusoidal drive. The maximum allowable source level for phase modulated pseudorandom noise of the type used in these tests is 140 decibels.

It is possible that further studies might reveal methods of reducing transient over-shoots in pulsed sinusoidal excitation and high peak to rms spring deflection ratios in pseudorandom noise excitation, thus increasing the allowable power input for both modes of operation.

RECOMMENDATIONS

It is recommended that additional experiments and analytical studies be conducted for the purpose of gaining a better understanding of the transient response characteristics of the ARTEMIS source as well as for high power acoustic sources in general. The yield from such a study would be an enhanced ability to specify time functions which have desirable signal characteristics while, at the same time, permitting the optimum acoustic source level from a particular projector. The high cost of acoustic intensity heightens the attractiveness of utilizing the full capability of a projector through signal design.

Fig. 1 - The completed ARTEMIS acoustic source installed aboard the USNS MISSION CAPISTRANO
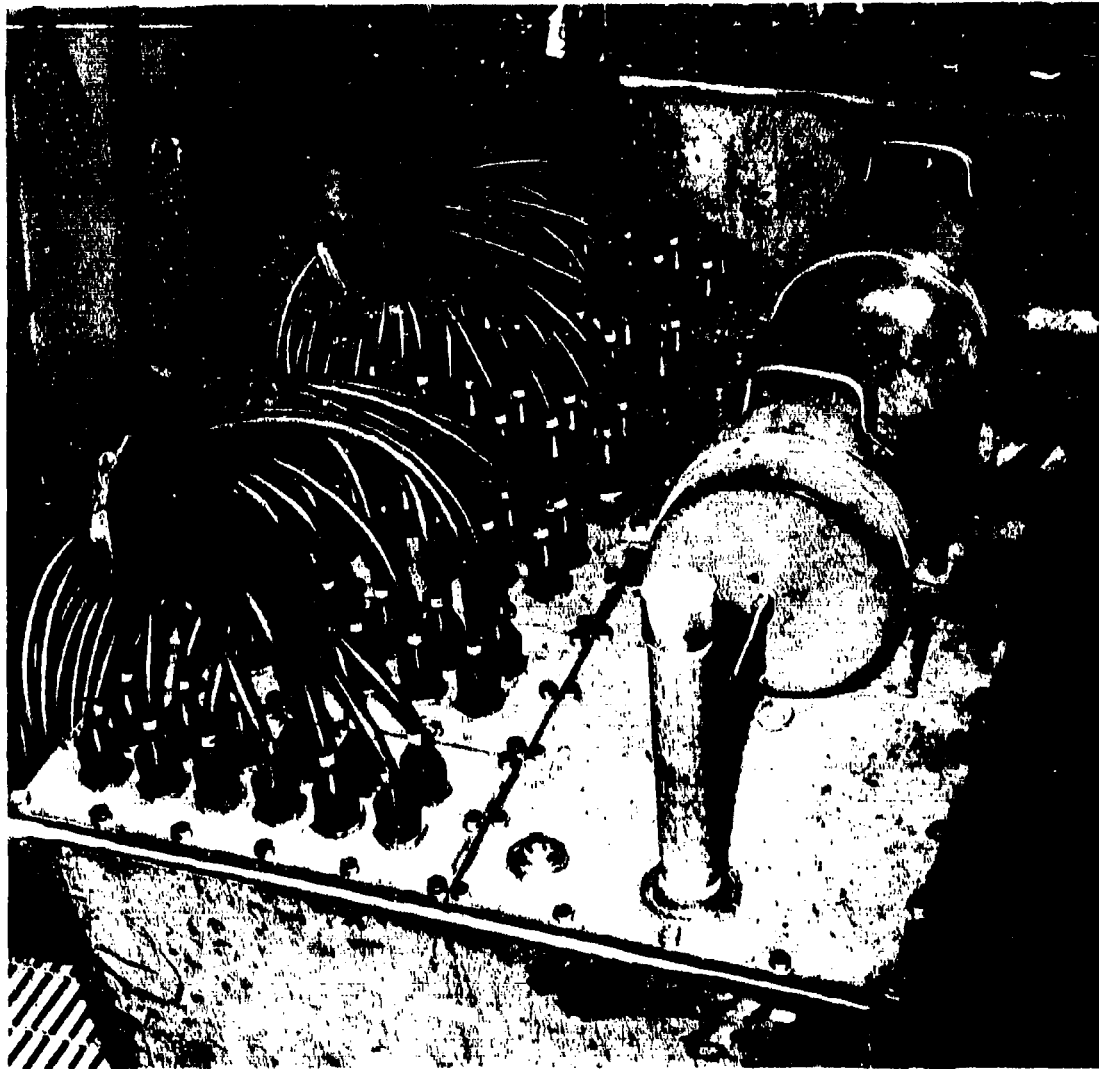
Fig. 2 - Paralleling transformer tank with pressure compensator
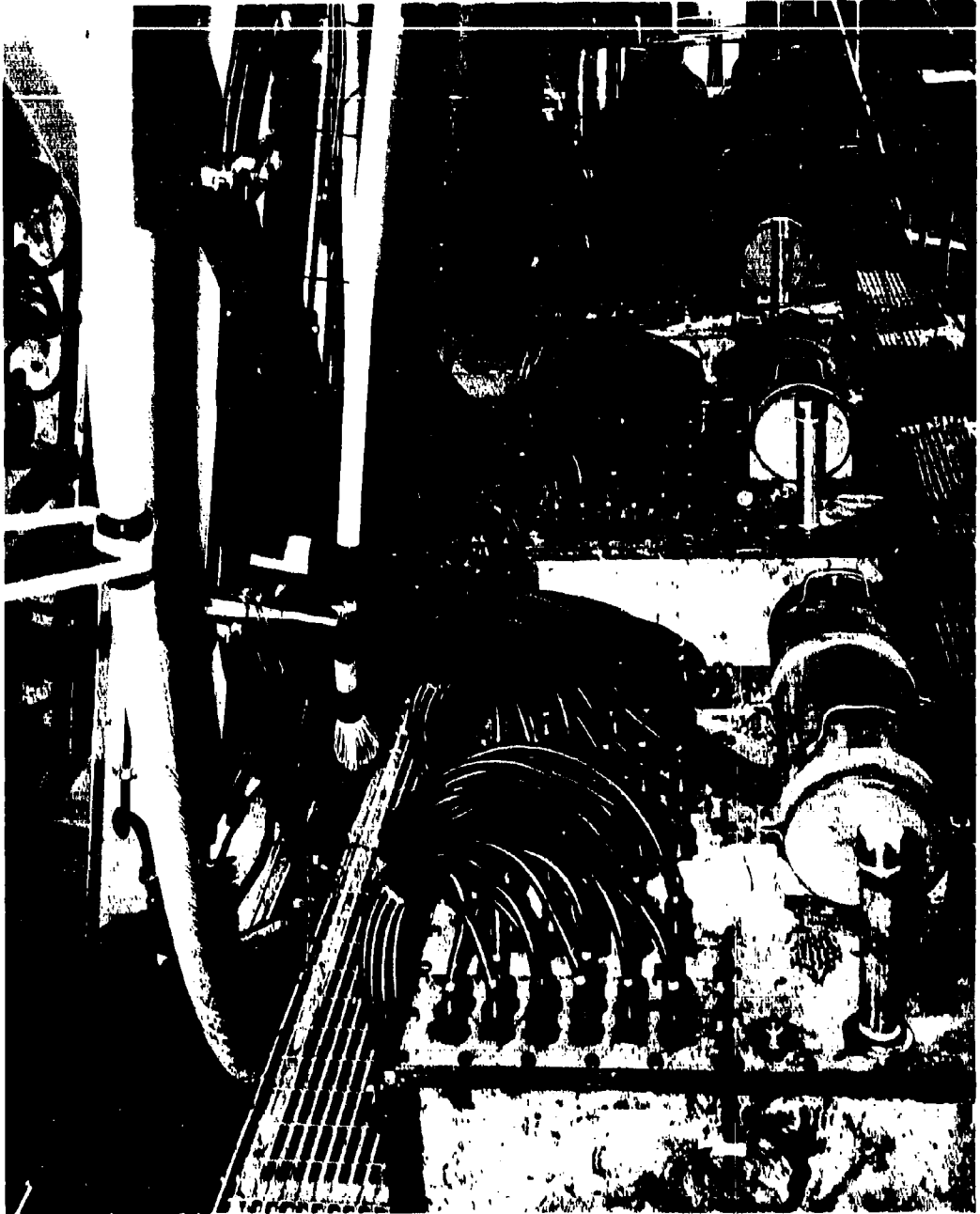
Fig. 3 - Paralleling transformer tanks installed on the ARTEMIS array

Fig. 4 - Module arrangement on the
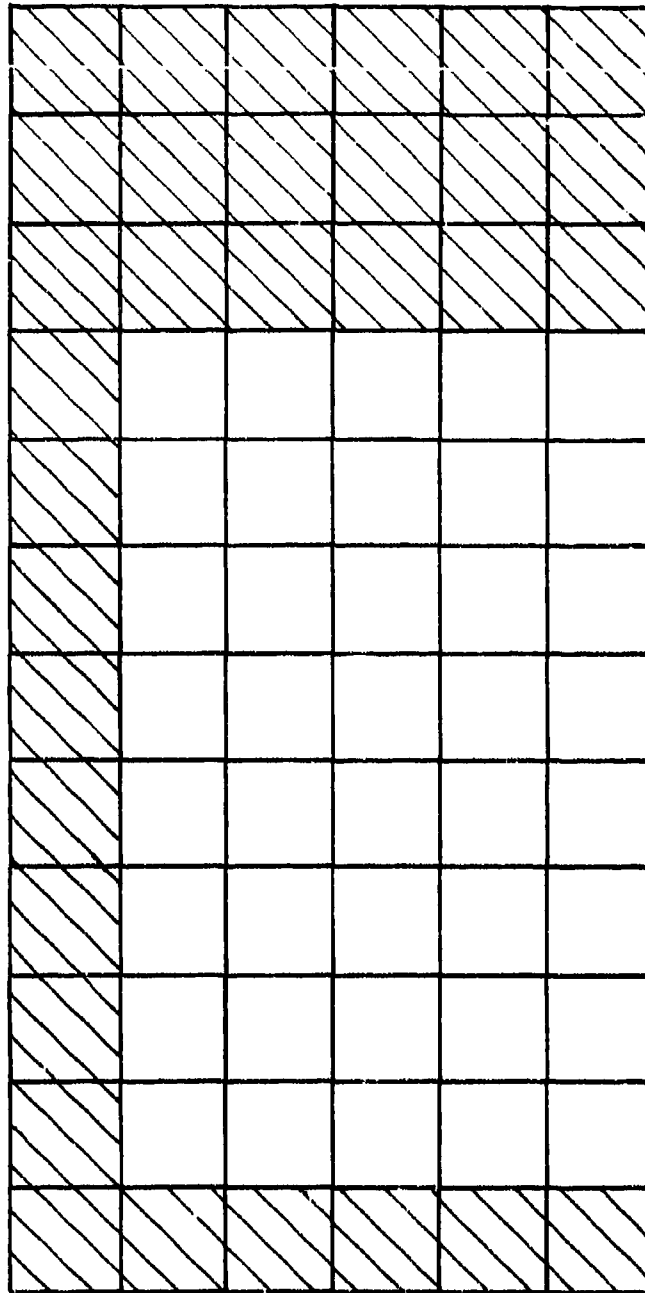ARTEMIS source. Shading indicates
test module positions.

Fig. 5 - Arrangement of elements in an
ARTEMIS transducer module. Shading
indicates location of specially instru-
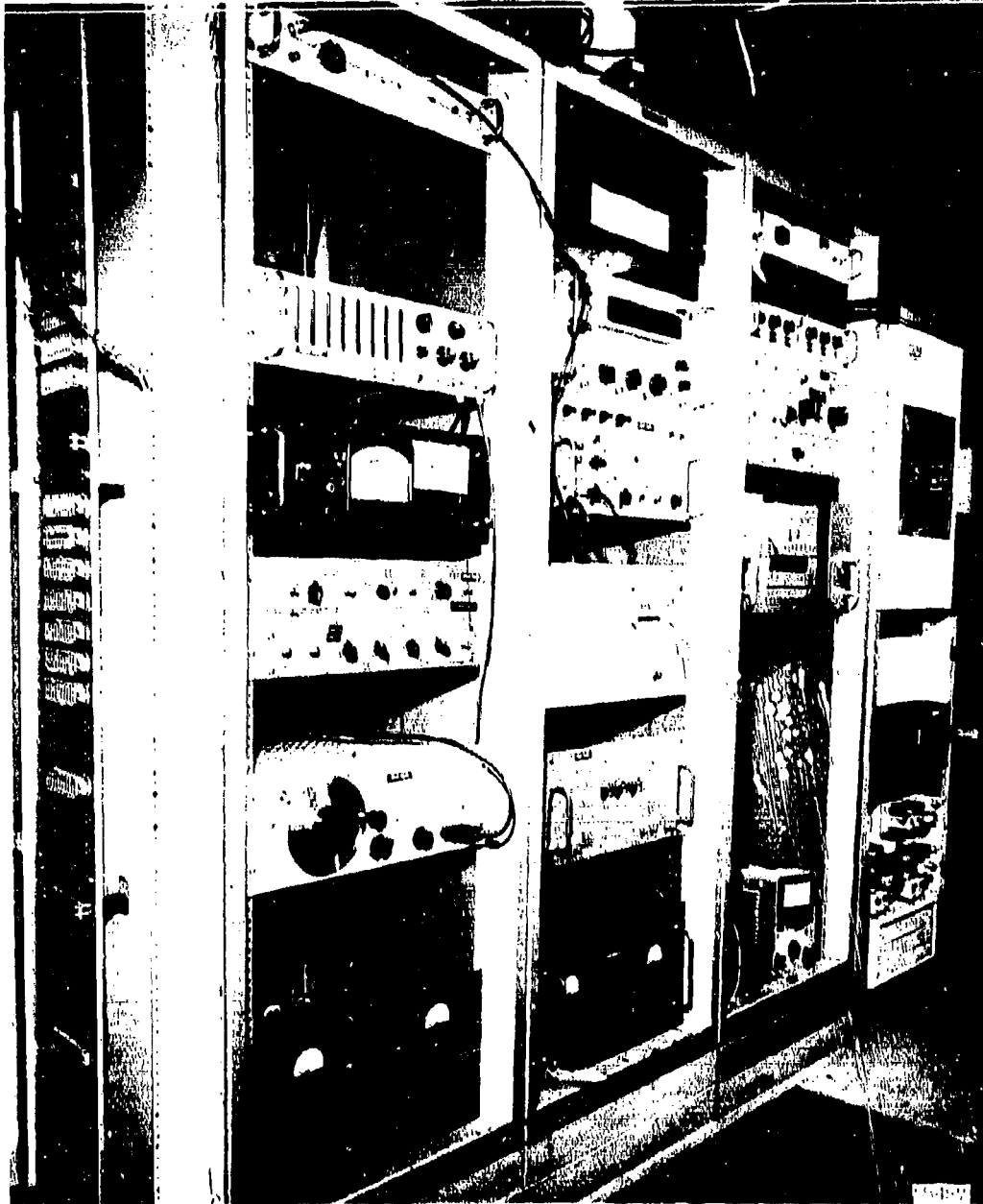mented elements in the test module.

Fig. 6 - View of test instrumentation in amplifier room
of MISSION CAPISTRANO
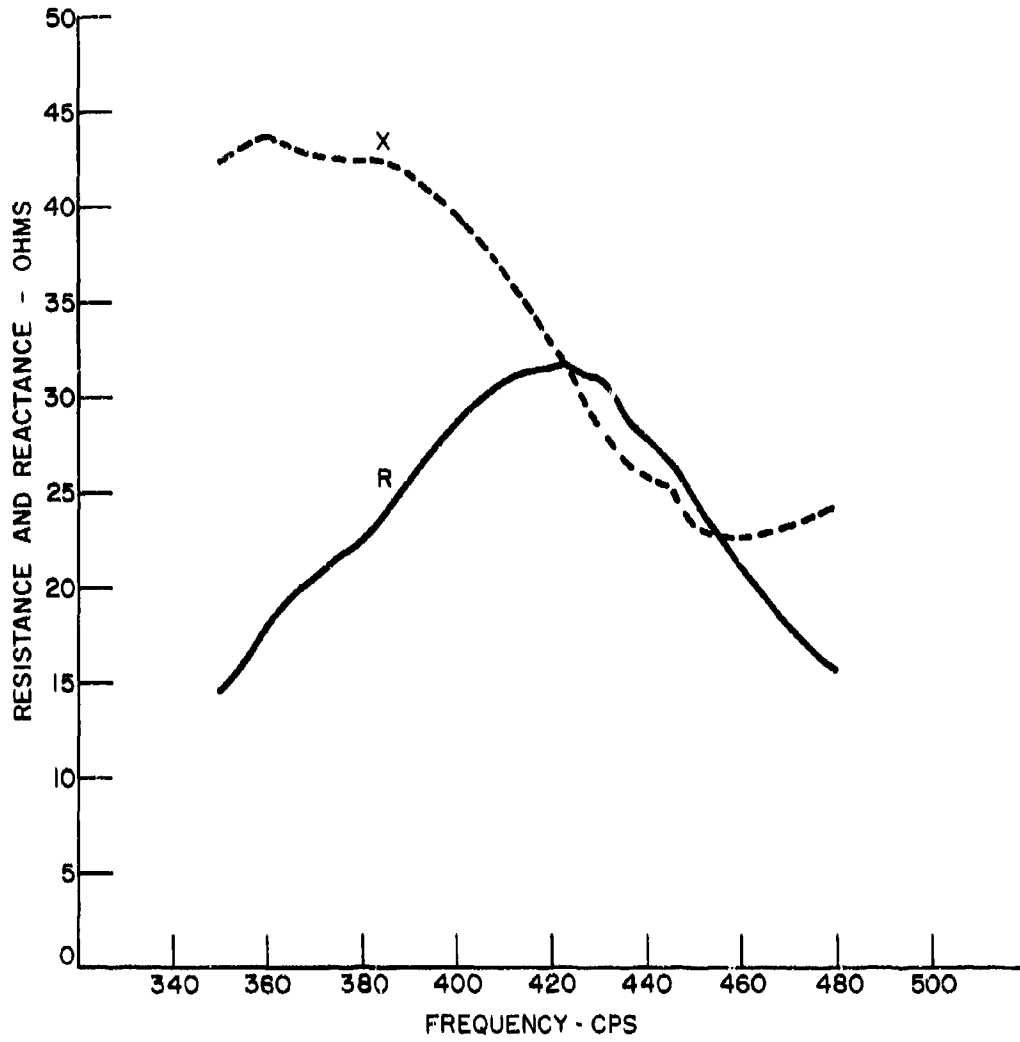
Fig. 7 - Resistive and reactive components
of transducer impedance
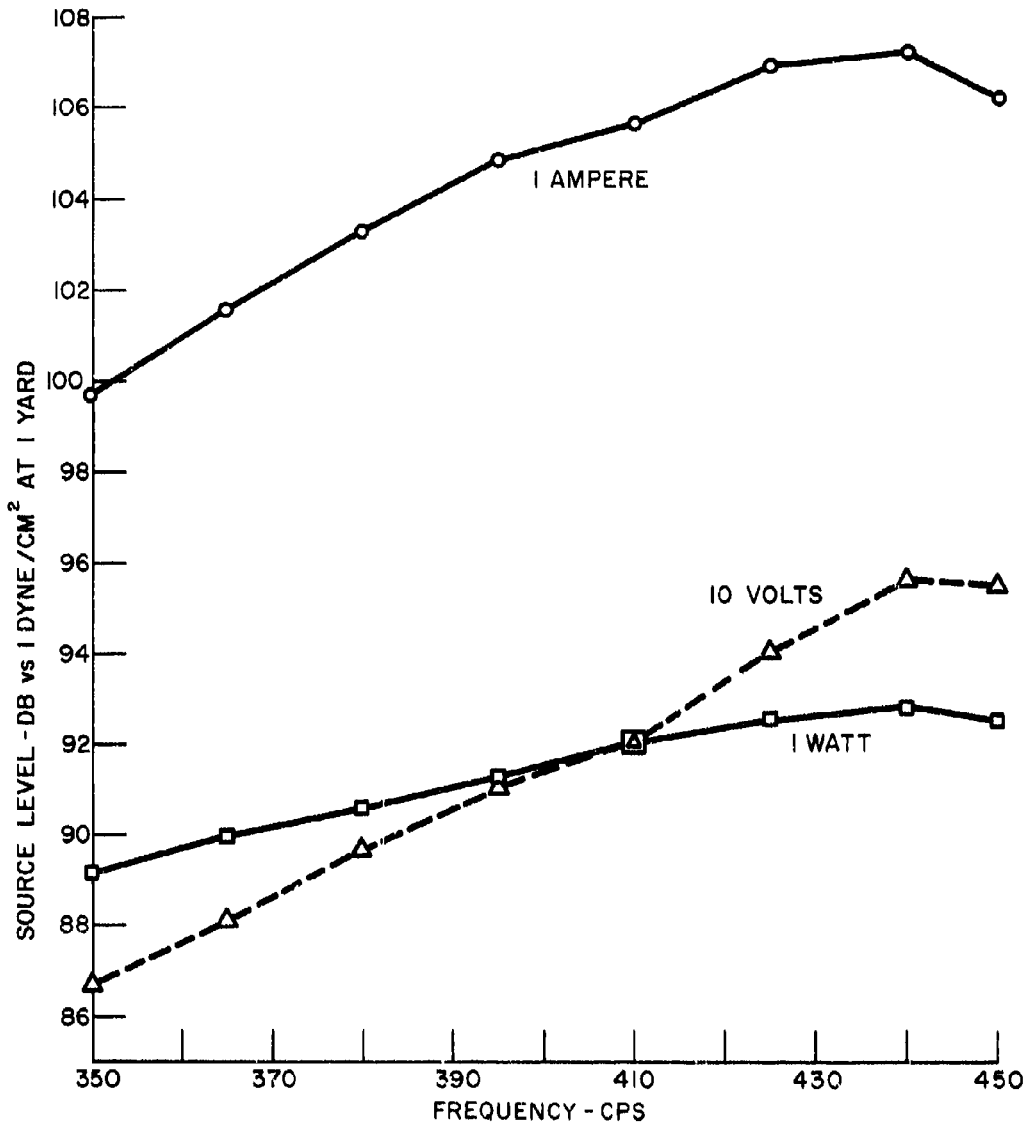
Fig. 8 - Current, power, and voltage response
of ARTEMIS acoustic source
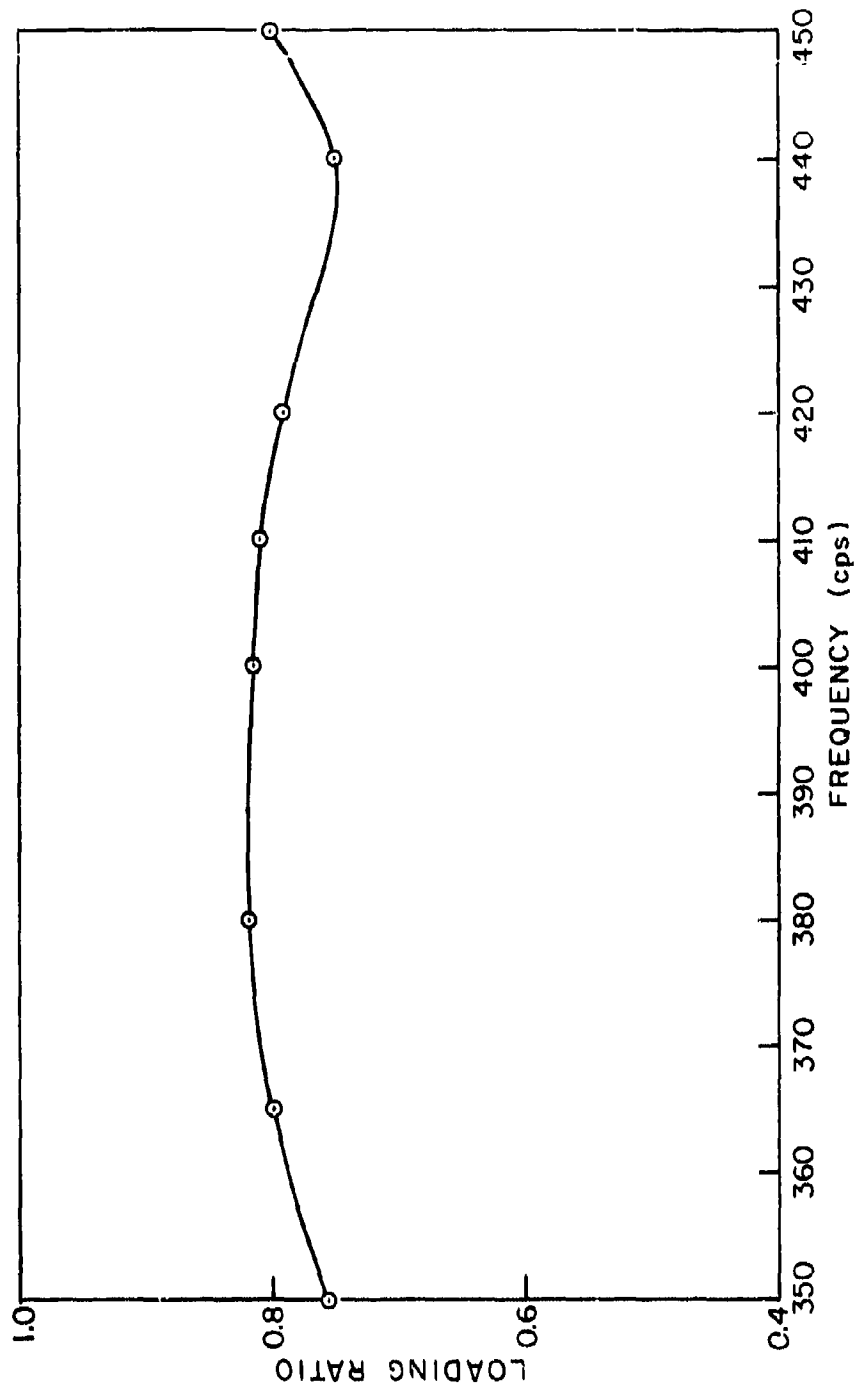
Fig. 9 - Loading characteristics of transducer array relative to unity pcA loading
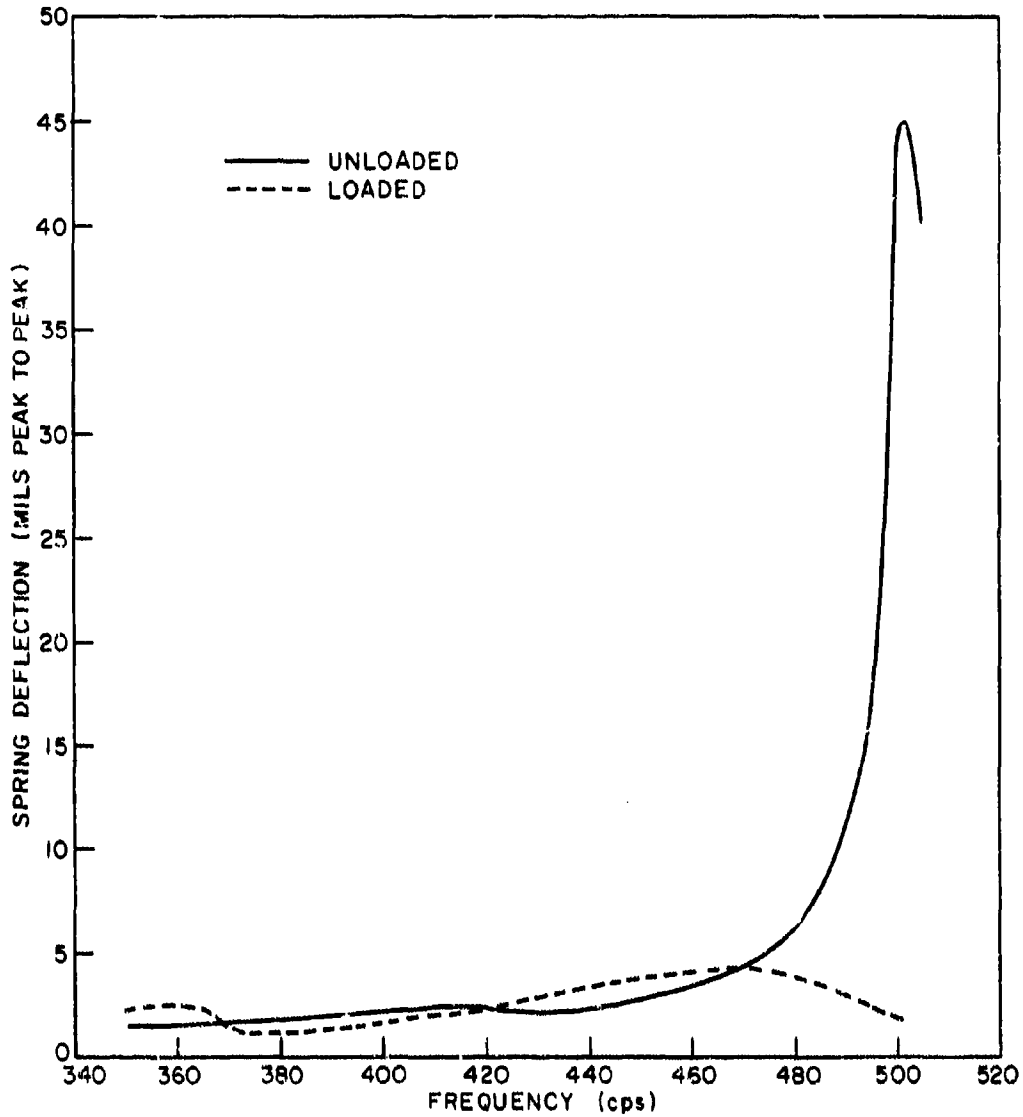
Fig. 10 - Comparison of spring deflections for a resistively loaded and an unloaded transducer element normalized to 100 volts across element input. A purely mass reactive loading would result in a large peak similar to the unloaded element but at a lower frequency.
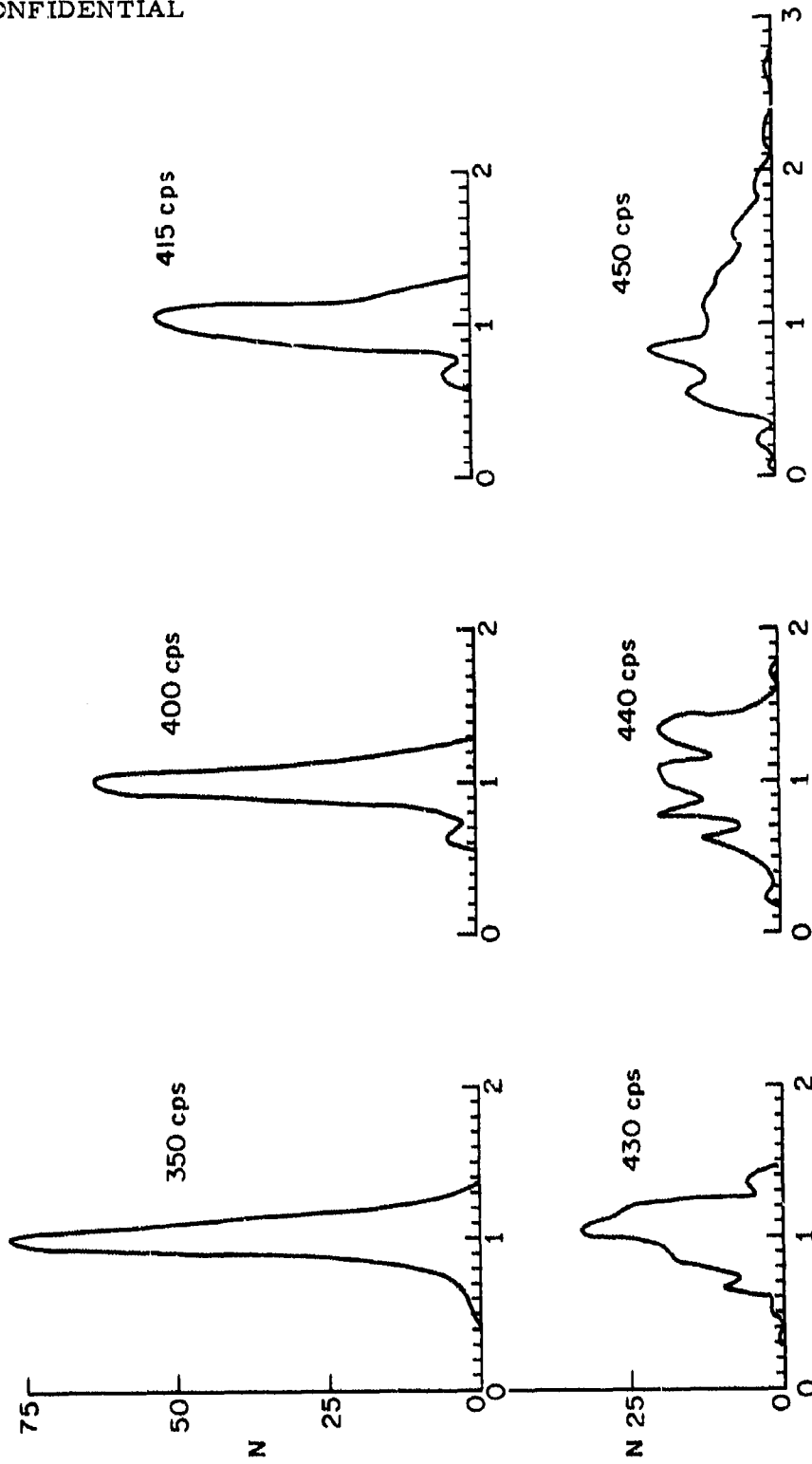
Fig. 11 - Distribution of displacements of the radiating faces of the elements relative to the mean displacement at each frequency
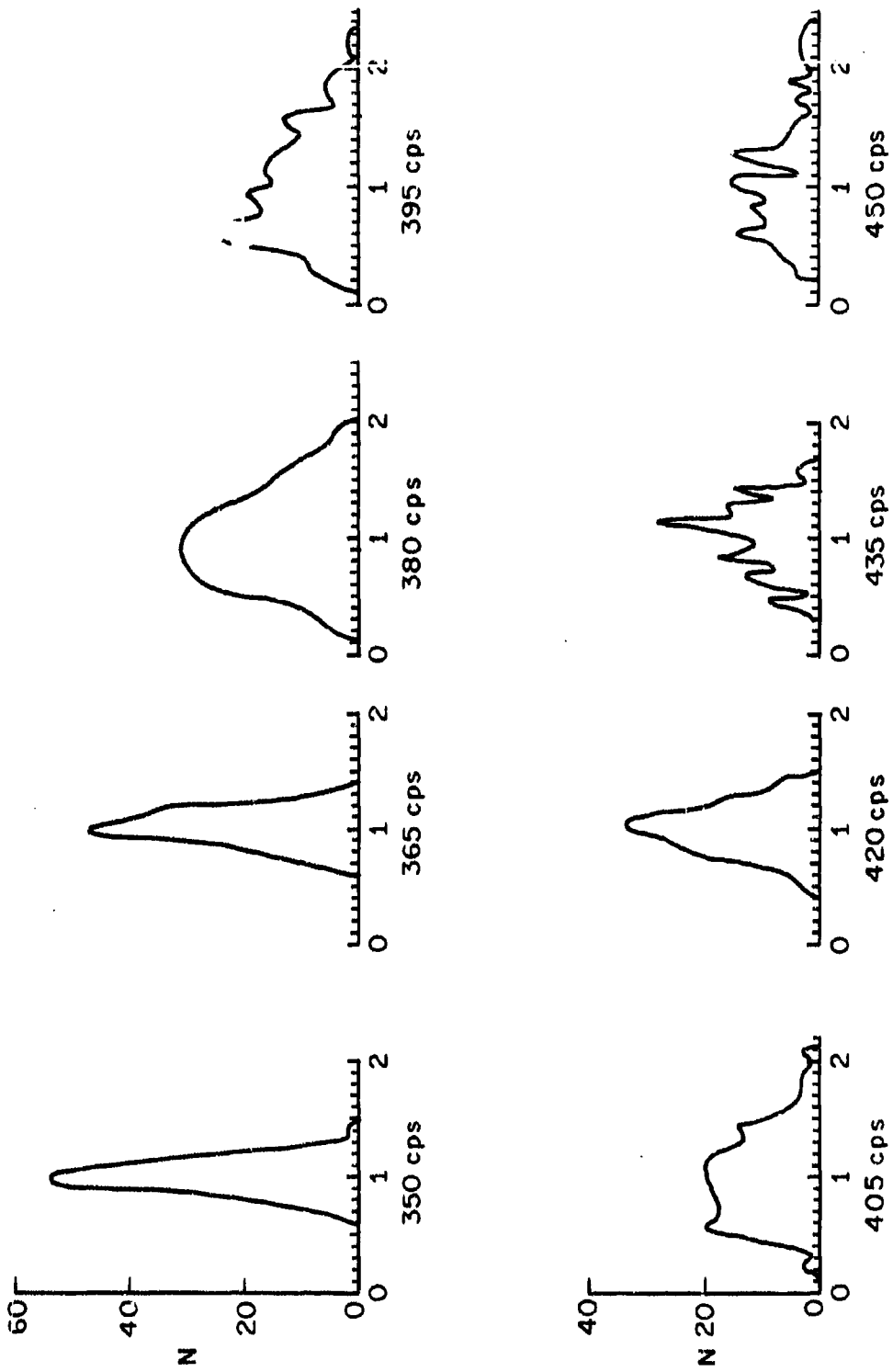
Fig. 12 - Distribution of transducer element spring deflections relative to the mean deflection at each frequency
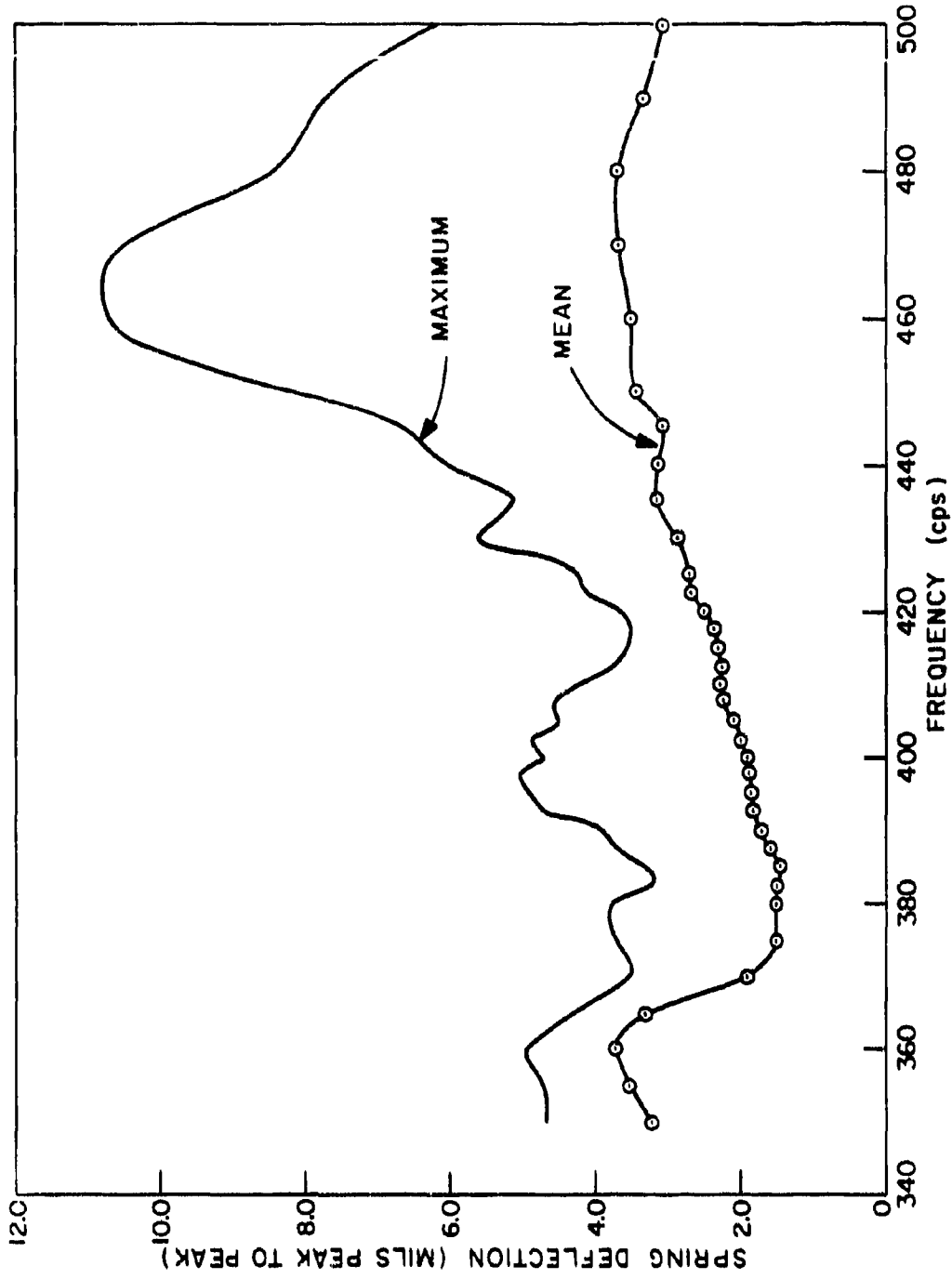
Fig. 13 - Mean and maximum spring deflections normalized
to a constant input power of 100 kilowatts
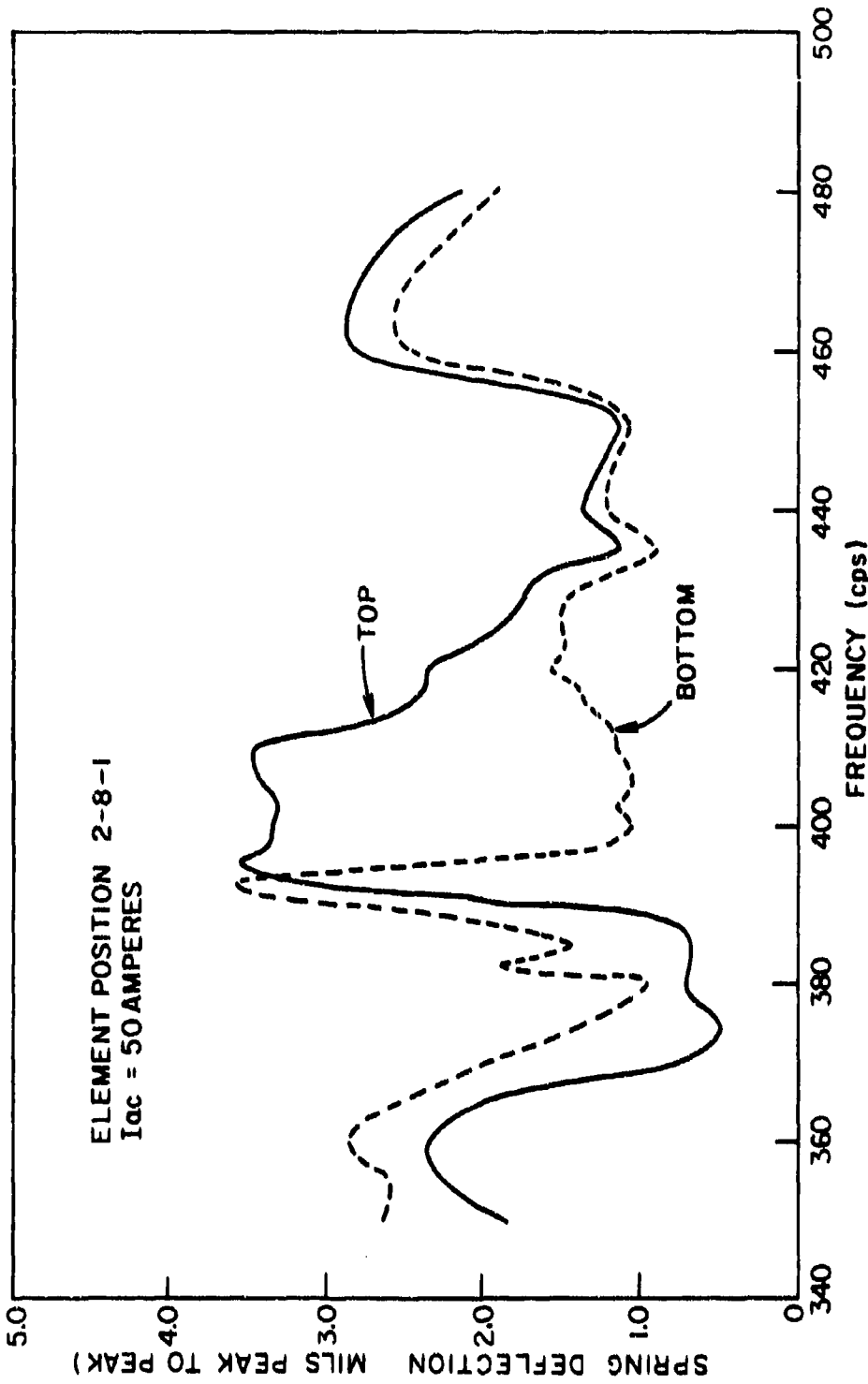
Fig. 14 - Deflections of the upper and lower springs in a transducer element illustrative of the frequency dependence for constant current input
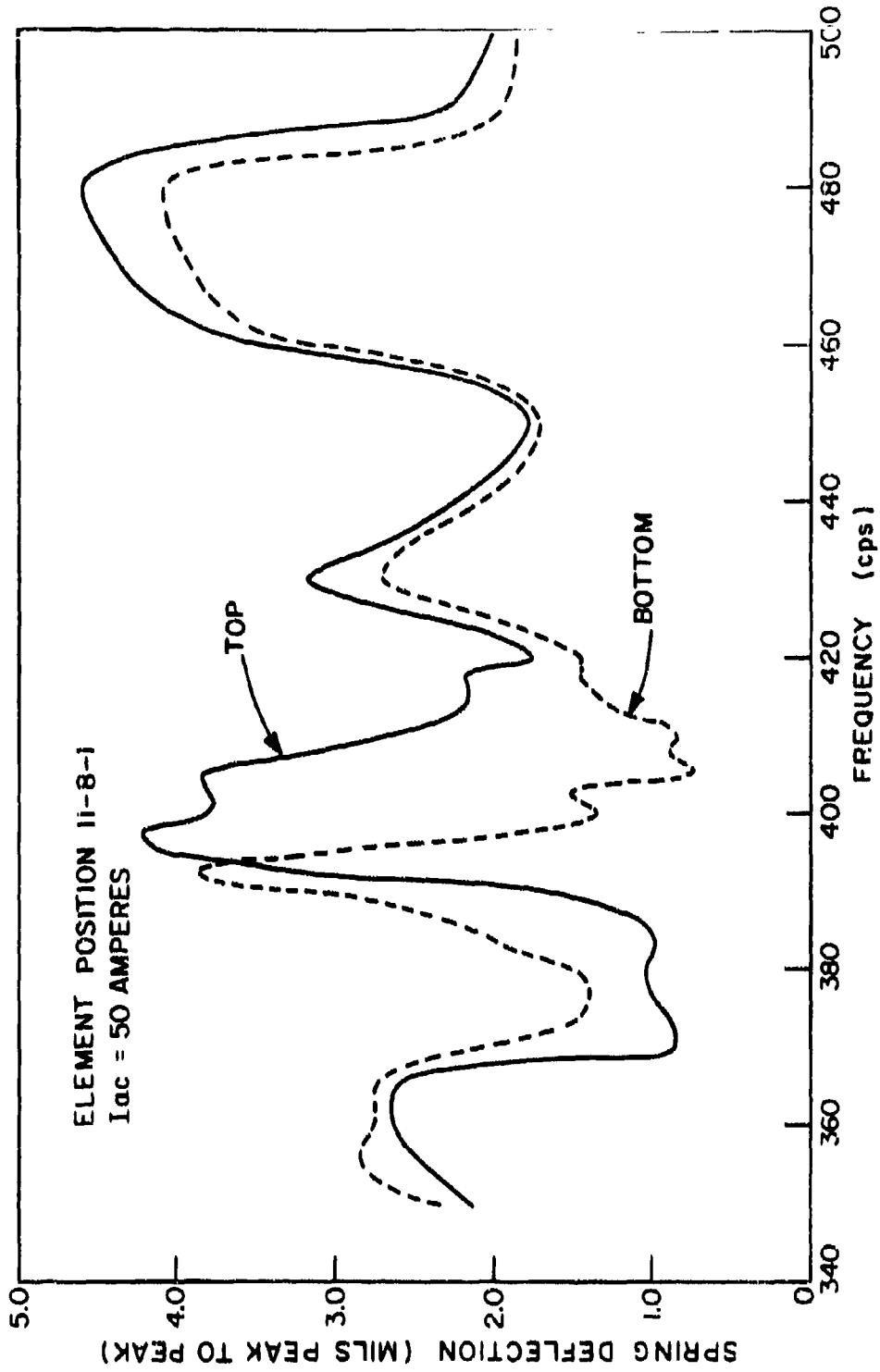
Fig. 15 - Deflections of the upper and lower springs in a transducer element illustrative of the frequency dependence for constant current input

ELEMENT II-3-I
Iac = 50 AMPERES

FREQUENCY (cps)

ROCKING ANGLE (MINUTES)
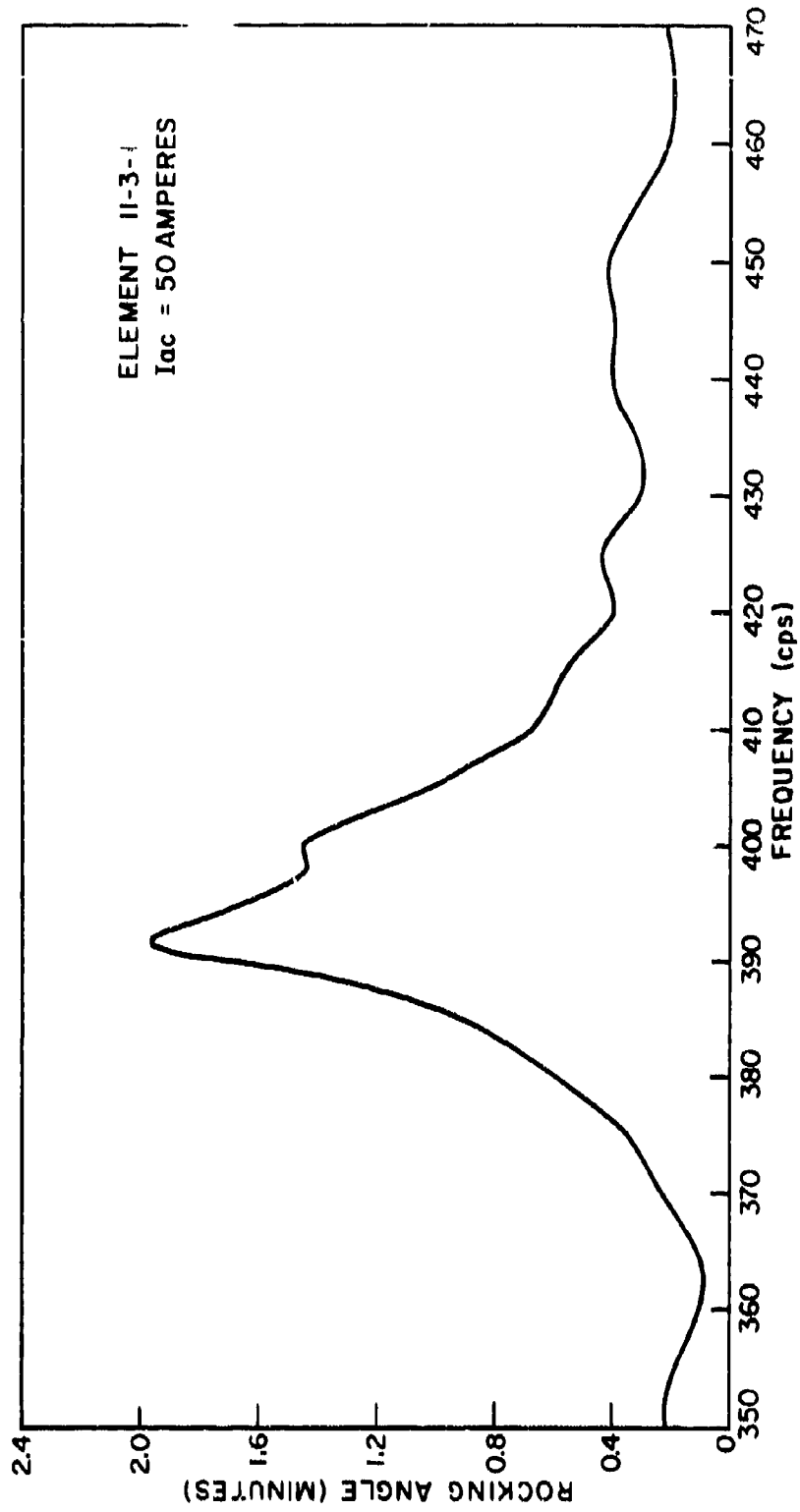
Fig. 16 - Rotary motion of the inner mass of a transducer element
illustrative of the frequency dependence

ELEMENT 2-8-1
Iac = 50 AMPERES

FREQUENCY (cps)

ROCKING ANGLE (MINUTES)
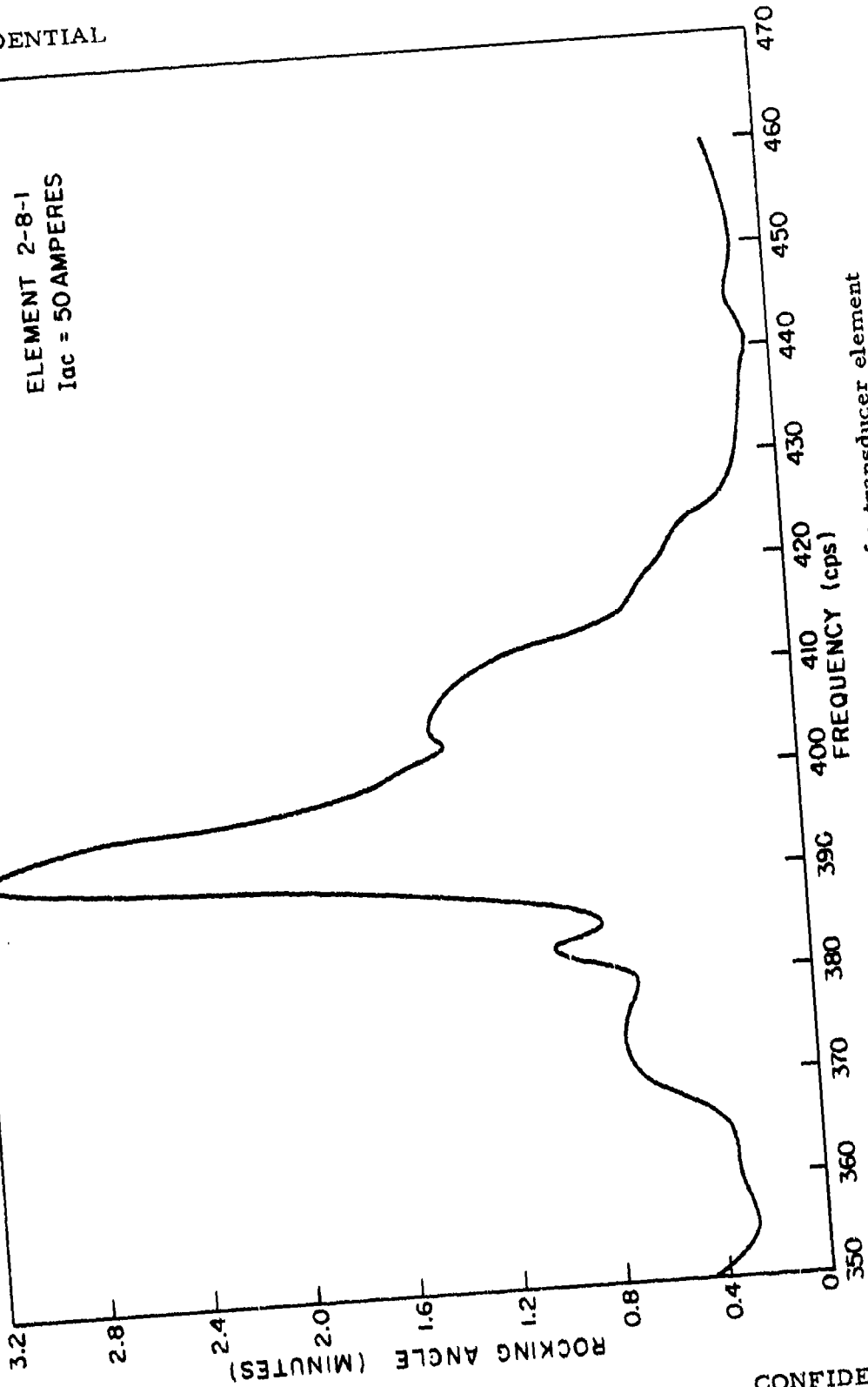
Fig. 17 – Rotary motion of the inner mass of a transducer element illustrative of the frequency dependence
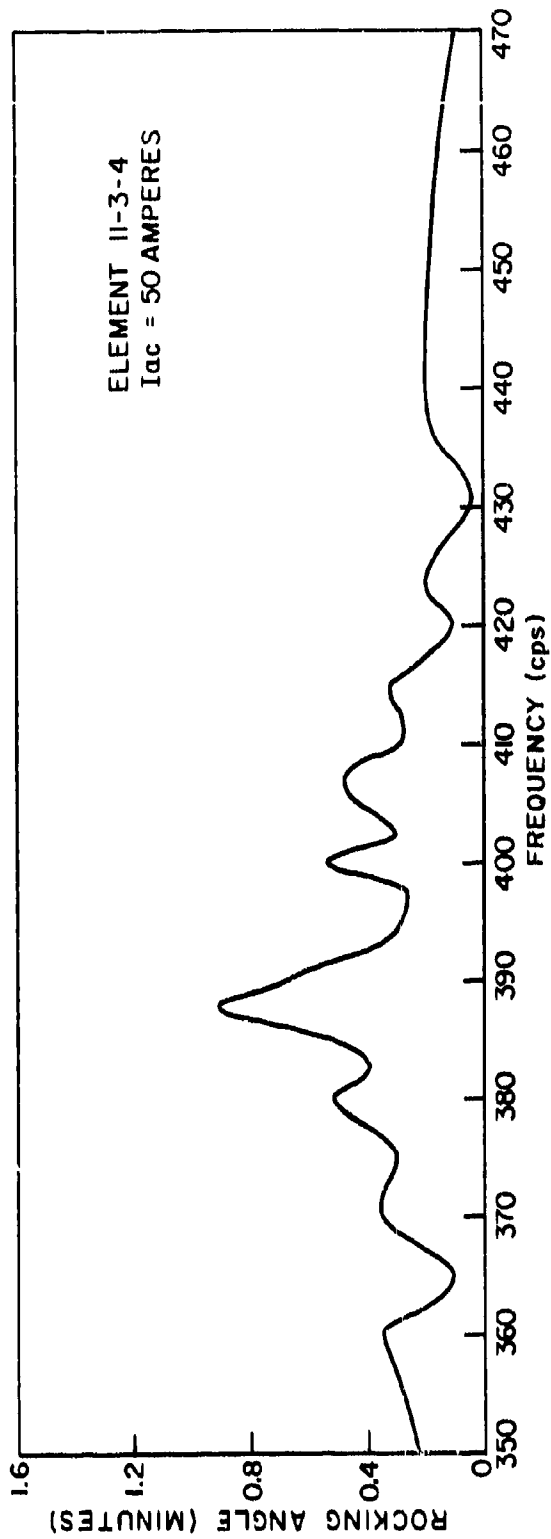
Fig. 18 – Rotary motion of the inner mass of a transducer element
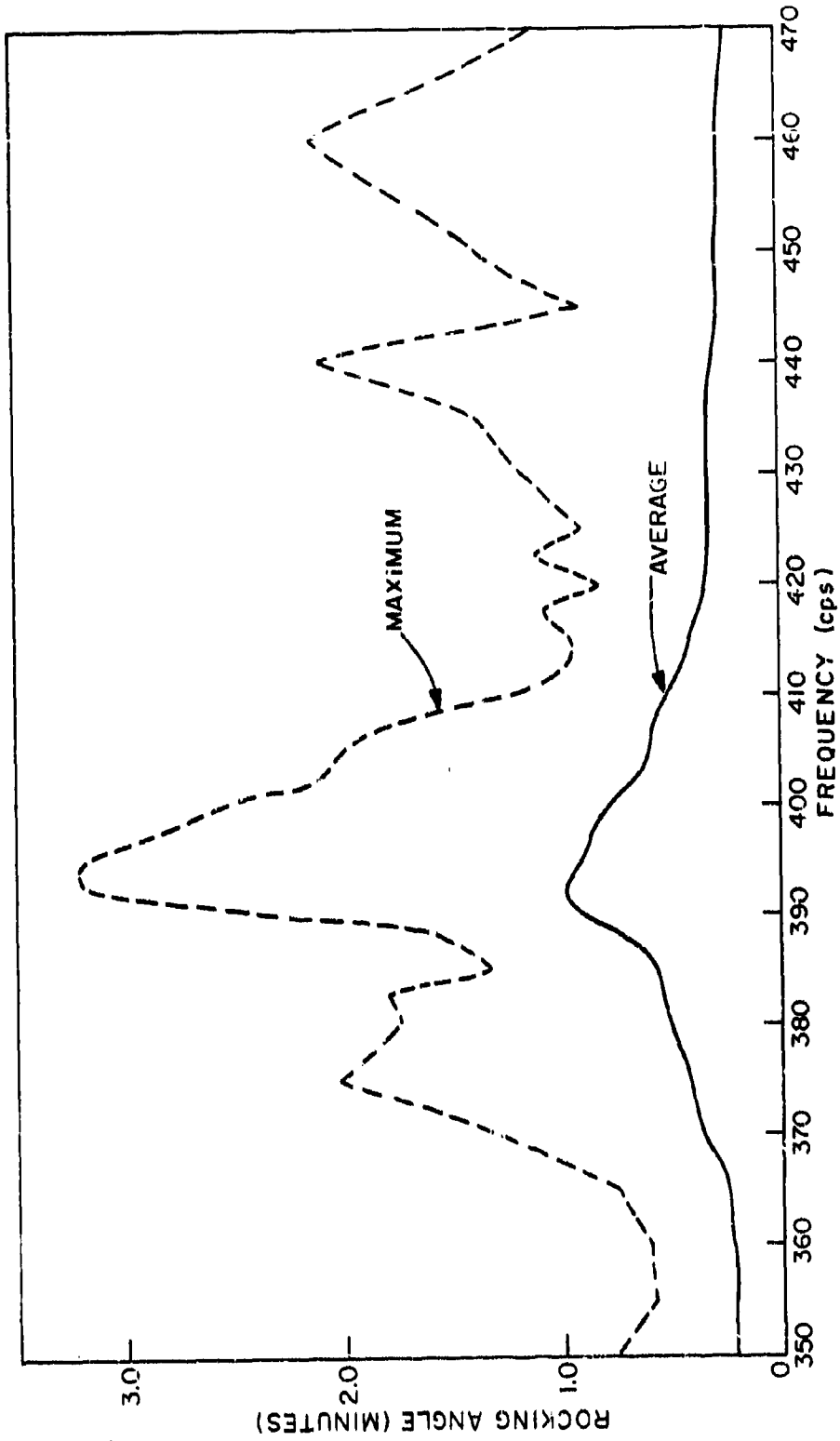illustrative of the frequency dependence
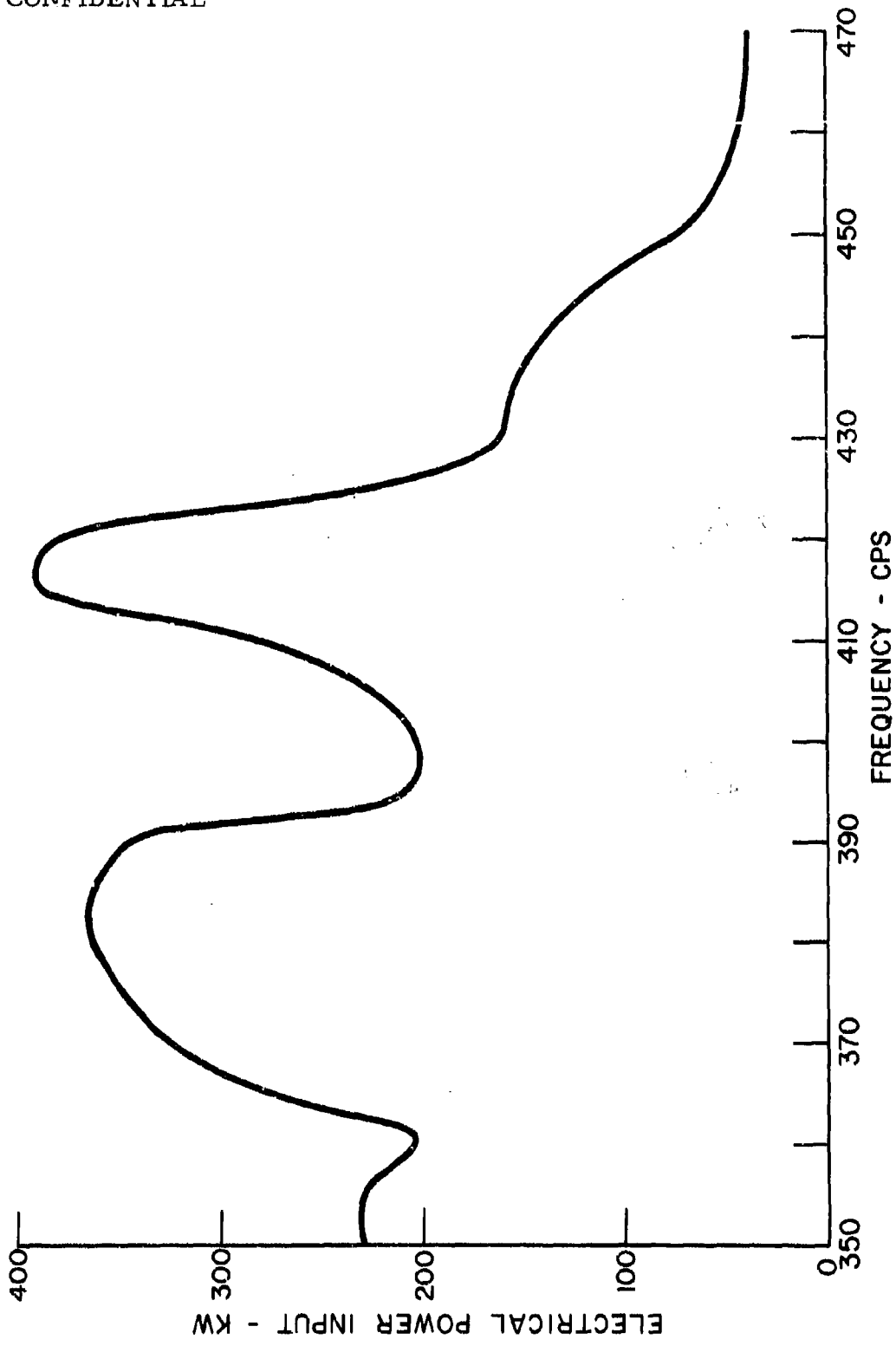
Fig. 19 - Average and maximum values of rocking angle for all sampled elements
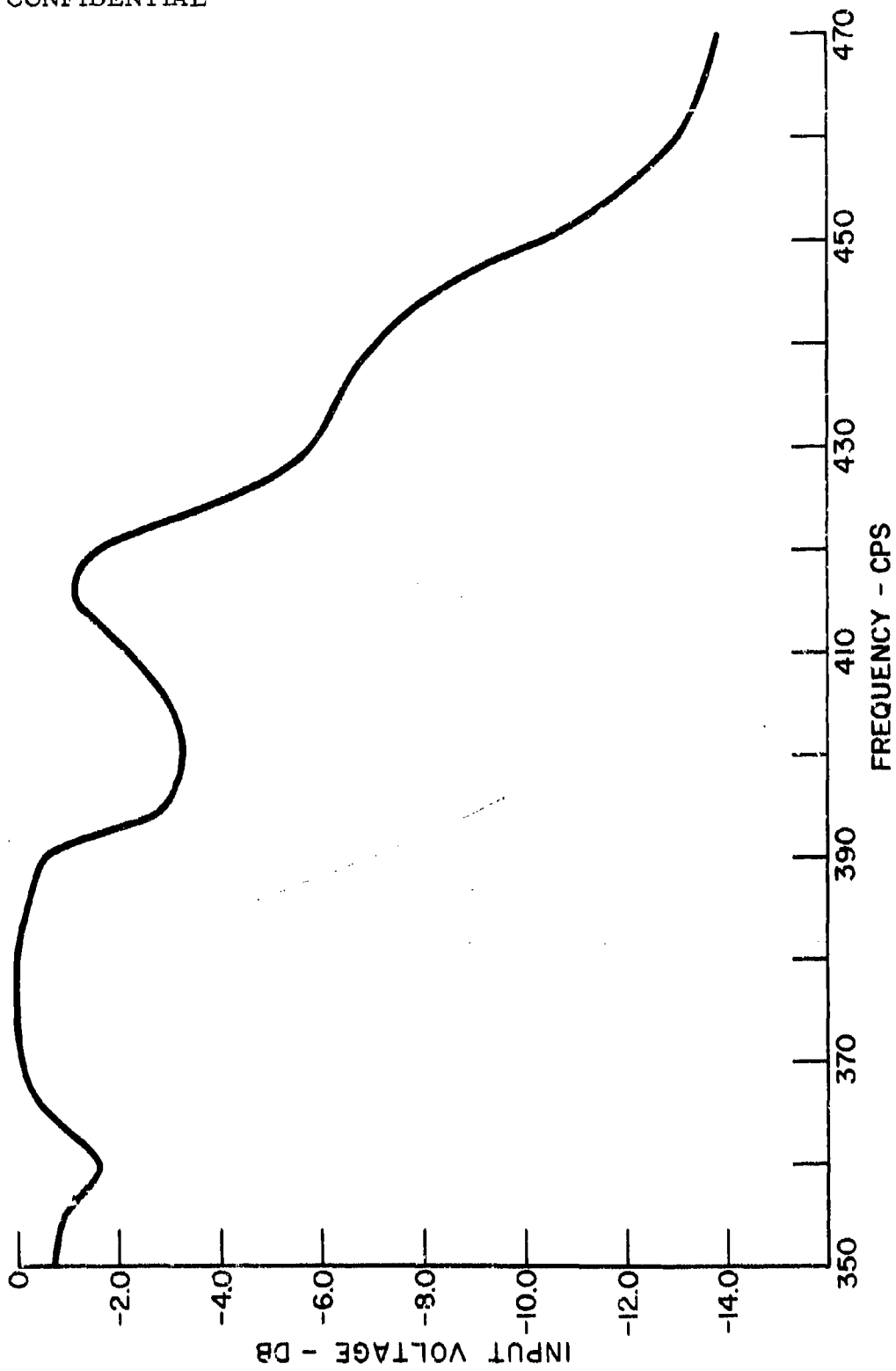
Fig. 20 - Maximum allowable power input to the completed ARTEMIS acoustic source

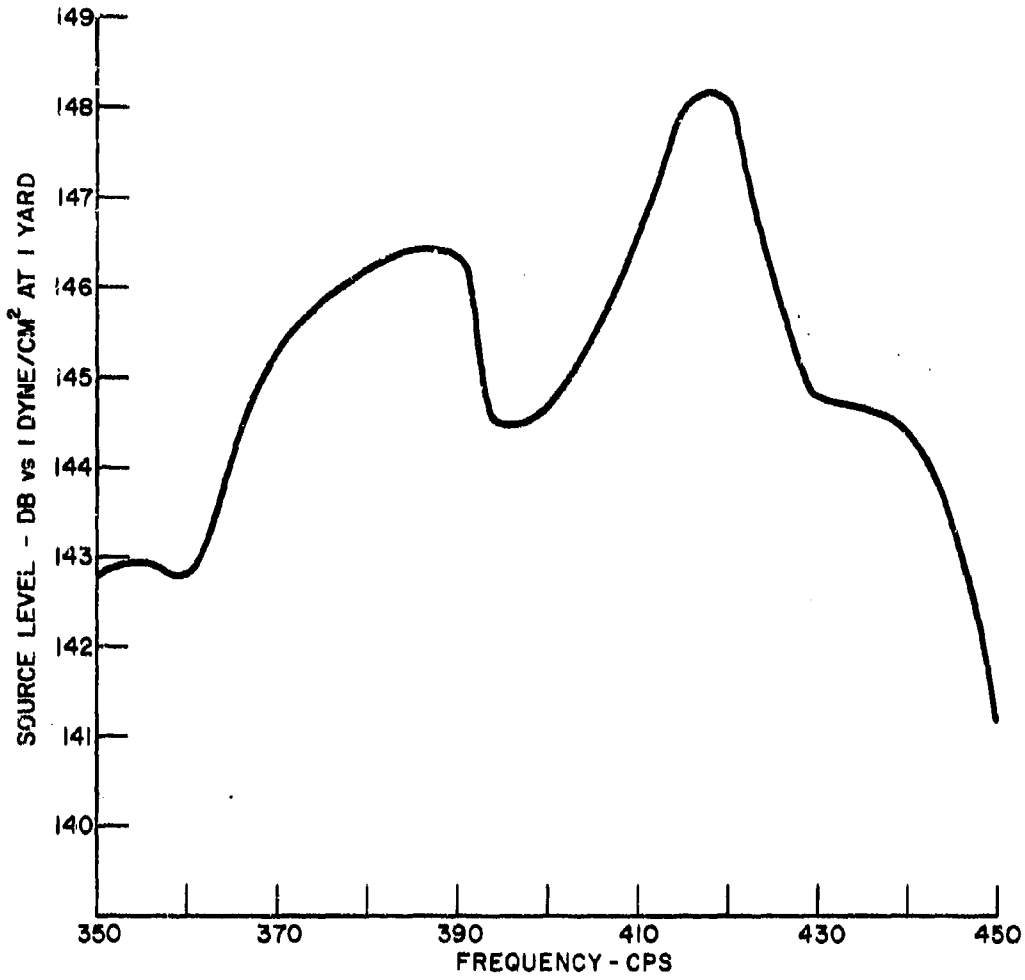Fig. 21 - Relative maximum allowable voltage input to the driver amplifiers for the ARTEMIS acoustic source

Fig. 22 - Maximum available source level from
the ARTEMIS acoustic source

UNITED STATES GOVERNMENT
Memorandum

7100-016

DATE: 22 January 2004

REPLY TO
ATTN OF: Burton G. Hurdle (Code 7103)

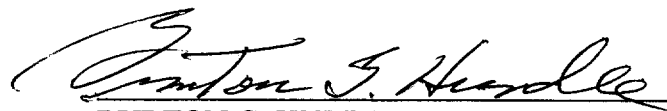**SUBJECT:**   REVIEW OF REF (A) FOR DECLASSIFICATION

TO: Code 1221.1

REF: (a) "Project ARTEMIS High Power Acoustic Source", A.T. McClinton, R.H. Ferris, W.A. Herrington, Sound Div., NRL Memo Report 1205, 3 Aug 1961 (U)
(b) "Project ARTEMIS High Power Acoustic Source Second Interim Report on Acoustic Performance", A.T. McClinton and R.H. Ferris, Sound Division, NRL Memo Report 1214, 19 September 1961 (U)
(c) "Project ARTEMIS High Power Acoustic Source Third Interim Report on Acoustic Performance", A.T. McClinton, R.H. Ferris, Sound Division, NRL Memo Report 1273, 23 April 1962 (U)
(d) "Project ARETMIS High Power Acoustic Source Effect of Transducer Element Electrical Connection on Interaction in a Consolidated Array", A.T. McClinton, Sound Division, NRL Memo Report 1323, 4 June 1962 (U)
(e) "Test of Project ARTEMIS Source", R.H. Ferris, Sound Division, NRL Memo Report 1648, 15 September 1965 (U)
(f) "Power Limitations and Fidelity of Acoustic Sources", R.H. Ferris and F.L. Hunsicker, Sound Division, NRL Memo Report 1730, November 1966 (U)
(g) "Project ARTEMIS Acoustic Source Acoustic Test Procedure", R.H. Ferris and C.R. Rollins, Sound Division, NRL Memo Report 1769, 5 June 1967 (U)
(h) "Calibration of the ARTEIS Source and Receiving Array on the Mission Capistrano", M. Flato, Acoustics Div., NRL Memo Report 2712, Dec 1973 (U)
(i) "Theoretical Interaction Computations for Transducer Arrays, Including the Effects of Several Different Types of Electrical Terminal Connections", R.V. Baier, Sound Division, NRL Report 6314, 7 October 1965 (U)
(j) "Project ARTEMIS Acoustic Source Summary Report", NRL Report 6535, September 1967 (U)

1. References (a) thru (j) are a series of reports on Project ARTEMIS Reports by the Sound Division that have previously been declassified.

2. The technology and equipment of reference (a) have long been superseded. The current value of these papers is historical

3. Based on the above, it is recommended that reference (a) be available with no restrictions.

BURTON G. HURDLE
NRL Code 7103

CONCUR:

E.R. Franchi   Date
Superintendent, Acoustics Division

CONCUR:

Tina Smallwood   Date
NRL Code 1221.1